ACS APPLIED MATERIALS & INTERFACES

Research Article

www.acsami.org

# EDTA-Induced Self-Assembly of 3D Graphene and Its Superior Adsorption Ability for Paraquat Using a Teabag

Yang Huang, Chaoran Li, and Zhang Lin*

State Key Laboratory of Structural Chemistry, Fujian Institute of Research on the Structure of Matter, Chinese Academy of Sciences, Fuzhou, Fujian 350002, People's Republic of China

Supporting Information

**ABSTRACT:** In the past two years, three-dimensional graphene (3DG) was introduced to the environmental treatment area as a promising new material. Despite much progress in its synthesis and applications, 3DG is still limited in terms of green large-scale synthesis and practical environmental applications. In this work, a 3DG synthetic method was developed at 95 °C in an EDTA-induced self-assembly process. Because little EDTA was found to be consumed during synthesis, which might be due to its great stability and poor reducibility, 3DG with complete structure can be successively obtained by reusing the EDTA solution more than 10 times. Furthermore, 3DG was found to possess a superior adsorption capacity of 119 mg $g^{-1}$ (pH 6.0) for paraquat, a highly toxic herbicide with positive charges and a conjugated system of $\pi$ bonds in its molecular structure. The adsorption capacity was much higher than those in classic paraquat adsorbents, such as clay and activated carbon. To address the problem of 3DG damage by stirring, a pyramid-shaped nylon teabag was adopted to protect the soft hydrogel during the repeated adsorption−desorption processes. After five cycles, the 3DG teabag still maintained 88% of the initial adsorption capacity. This facile method may be easily applied in other environmental treatment conditions.

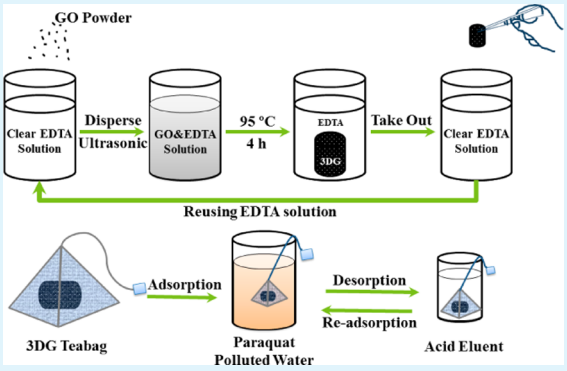


**KEYWORDS:** *three-dimensional graphene, EDTA, self-assembly, green synthesis, paraquat, teabag recycling*

## 1. INTRODUCTION

In the past few years, a type of monolith material called three-dimensional graphene (3DG) quickly drew extensive research interest,[1−4] especially in environmental treatment.[5−7] This graphene-based monolith usually has a low-density porous structure which allows diffusion of ions and molecules throughout.[6,8] More importantly, compared to graphene, 3DG can effectively avoid layer−layer aggregation and retain the large specific surface, not to mention the convenience it brought to separation and recycling processes. Increasing studies have shown the good adsorption capability of 3DG for pollutants such as heavy metal ions,[5] organic solvents[7,9,10] and dyes.[11,12] For wider applications[13,14] of 3DG in environmental treatment, a feasible synthetic method appropriate for adsorption is needed.

So far, two synthetic methods[2] of 3DG have been developed—template growth and free-standing. The template growth method[15−17] utilizes chemical vapor deposition (CVD) to grow graphene structures directly on the sacrificed template, which requires precise control of temperature and atmosphere. In the direct drying technique,[5] one of the free-standing methods, 3DG is synthesized by vacuum freeze-drying or critical point drying. In comparison, self-assembly, another free-standing method, is attracting more attention for its ease of operation. For example, Shi et al.[18] obtained pure 3DG structure through hydrothermal reduction self-assembly of graphene oxide (GO). However, this method requires high temperature and pressure and can hardly realize large-scale production as limited by the size of hydrothermal reactors. Zhao et al.[19] and Zhao et al.[20] used linking agents such as pyrrole and thiourea to achieve carbon sponges with a reversible compression, yet also under high temperature and pressure conditions. Moreover, the toxic linking agents would eventually enter the 3DG structure. There was another type of synthetic method[21,22] using chemical reducing agents such as $NaHSO_3$, $Na_2S$, HI, $NaBH_4$, or ascorbic acid to reduce GO and yield 3DG under rather low temperatures (90−95 °C). This type of methods has great potential in environmental applications for its low requirements of equipment, mild synthetic conditions, and convenience for large-scale production. Nevertheless, the reducing agents mentioned above are usually unstable and sensitive to water, oxygen, or light, which increases consumption and raises costs. Furthermore, most of them are harmful to the ecosystem. It is therefore a challenge to develop a synthetic method which can produce "green" 3DG in

Received: July 25, 2014
Accepted: October 31, 2014
Published: October 31, 2014

  

large scale under mild conditions without introducing any unstable or poisonous agents.

Besides synthesis, problems also exist in the 3DG adsorption process. First, 3DG used in the adsorption of pollutants in water is usually in the form of hydrogel. Soft hydrogel could easily be damaged under stirring, losing its advantageous ability to recycle. Without stirring, however, it would take much longer to reach the adsorption equilibrium. Moreover, how to realize convenient separation of 3DG after adsorption is another question worth considering. It is undesirable to manually pick 3DG one by one, especially when facing large-scale adsorbents. Traditional means of separation such as filtration and centrifugation may not only break the 3D structure causing a decline in adsorption efficacy but also complicate the separation step. It is reported that embedding magnetic iron cores into 3DG can realize a quick and easy separation.[23] However, this approach limits its application in acidic pollutants or regeneration systems with acidic eluent. Therefore, an easy universal separation method that can protect the 3DG structure is strongly desired.

Ethylenediaminetetraacetic acid (EDTA) is a cheap and safe chemical compound that is widely used in various fields from household chemicals to rubber production. In this work, we attempted to obtain the 3DG structure at 95 °C through a self-assembly method involving EDTA. Considering that most of EDTA might remain unused due to its great stability and poor reducibility, the EDTA solution was reused in a successive 3DG synthesis process. Next, we investigated the adsorption efficacy of 3DG on pesticide paraquat (1,1′-dimenthyl-4,4′-bipyridyl dichloride). This was the first time 3DG was applied in the treatment of an agricultural organic pollutant. As one of the most widely used herbicides, paraquat is famous for its high toxicity and has been strictly limited in many countries and areas such as the United States, New Zealand, and Europe.[24,25] Paraquat can lead to serious water pollution because it is highly soluble in water and might accumulate in the environment.[26] At present, the classic adsorbents for paraquat removal are mainly limited to clay,[27−29] earth,[30,31] and activated carbon,[24] most of which showed rather poor performance. Recently, Hsu et al.[32,33] and Rongchapo et al.[26] used modified rice husk and zeolite-NaY/aelite-NaBEA as paraquat adsorbents, both showing good performances. Becaucsce paraquat possesses positive charges and an extended system of conjugated $\pi$ bonds, good interactions with graphene structures in 3DG are possible. In this study, we report a 3DG recycling strategy using a teabag, which is easy to operate and can possibly lead to extensive applications.

## 2. EXPERIMENTAL SECTION

**2.1. Materials.** All chemicals were reagent-grade and used without further purification. Graphite and paraquat were purchased from Alfa Aesar and Aladdin Reagent (Shanghai) Co., Ltd., respectively. Sulfuric acid ($H_2SO_4$), hydrochloric acid (HCl), hydrogen peroxide ($H_2O_2$), potassium permanganate ($KMnO_4$), and sodium nitrate ($NaNO_3$) were purchased from Sinopharm Chemical Reagent Co., Ltd., of China. The nylon teabag was from Lipton. All solutions were prepared using deionized (DI) water.

**2.2. Preparation of 3DG-Based Macrostructure and Reuse of EDTA.** GO was prepared from the pristine graphite using the modified Hummers method.[34] In a typical synthesis procedure, 15 mL of GO suspension with a concentration of 2 mg $mL^{-1}$, 5 mL of deionized water, and a certain amount of EDTA (0−5 mmol) were first mixed. After sonication for 10 min, the mixed solution was heated to 95 °C using an oil bath, and it was allowed to stand for 4 h. The as-obtained hydrogel was dialyzed in pure water for over 4 days, followed by freeze-drying to obtain the aerogel for further characterization. To reuse the residual EDTA solution, GO powder was dispersed into solution followed by sonication with a concentration of 2 mg $mL^{-1}$. After the heating synthetic procedure, 3DG hydrogel was taken out, and new GO powder was dispersed into the EDTA solution for the next cycle.

**2.3. Adsorption Experiments.** Adsorption experiments were performed at room temperature. Paraquat solutions (100 mL) with desirable concentrations were used for each adsorption experiment. The dosage of the 3DG macrostructure was 19 mg for each solution under continuous stirring.

*2.3.1. Adsorption Kinetics.* For kinetic studies, aliquots of 2 mL were extracted from paraquat solutions (20 and 50 mg $L^{-1}$, pH 6.0) at appropriate time intervals and then filtered by membrane filters (0.22 $\mu$m). The filtrate was immediately analyzed for its paraquat concentration using a Shimadzu UV-2550 double monochromatic UV visible spectrophotometer at the wavelength of 257 nm.

*2.3.2. Adsorption Isotherms.* 3DG samples were immersed in paraquat solutions of different concentrations (5, 20, 50, 100, and 400 mg $L^{-1}$, pH 6.0) and stirred for 24 h, which was found to be sufficient time for the mixture to reach equilibrium. After reaching equilibrium, the solution was extracted, filtered, and measured, as detailed above, and the adsorption capacity of the 3DG macrostructure was calculated. The adsorption capacity of 3DG at pH 12.0 was obtained by employing 3DG immersing in 400 mg $L^{-1}$ paraquat at pH 12.0 for over 24 h, assuming the paraquat removal was equal to $Q_e$.

*2.3.3. Effect of pH.* The adsorption capacities of 3DG were tested at different pHs. The pH of the paraquat solution was adjusted to 0, 2.7, 6.0, 10.0, and 11.6 with 1 M NaOH or 1 M HCl. A pH meter was used for pH measurement.

*2.3.4. Preparation of the 3DG Teabag and the Regeneration Experiment.* The 3DG teabag was made by simply putting 3DG into the nylon teabag and sealing the teabag with heat. In a typical regeneration process, the 3DG teabag was first soaked in 100 mL of 50 mM paraquat solution (pH = 12). After reaching equilibrium (~6 h in our case), the teabag was lifted and put into 10 mL of acidified water (pH = 0) for desorption until equilibrium. Then, the teabag was lifted again and washed with water until pH = ~7 for the next round of recycling.

**2.4. Characterization.** The phases of the samples were identified by the XRD patterns obtained on a PANalytical X'Pert PRO diffractometer with Cu K$\alpha$ radiation (40 kV, 40 mA) in the continuous scanning mode. The $2\theta$ scanning range was from 5° to 85° in steps of 0.017° with a collection time of 20 s per step. The morphology and size of the solid product were characterized on a JSM-6700F scanning electron microscopy equipped with an Oxford INCA energy dispersive X-ray spectroscopy (EDS). The specific surface area of the sample was measured with an accelerated surface area and porosimetry analyzer (Micromeritics, ASAP 2020). Fourier transform infrared spectroscopy (FTIR) and X-ray photoelectron spectroscopy (XPS) analysis were used for the determination of functional groups. The spectra were recorded on a PerkinElmer Spectrum One spectrometer and an ESCALAB 250 photoelectron spectroscopy (Thermo Fisher Scientific, Inc.) at $3.0 \times 10^{-10}$ mbar with monochromatic Al K$\alpha$ radiation (E = 1486.2 eV).

## 3. RESULTS AND DISCUSSION

**3.1. Synthesis and Characterization.** Figure 1a−f shows photos of 3DG synthesized in EDTA solutions at various concentrations. It can be observed that in the present of EDTA, GO shrunk into a black monolith when heated and floated in the clear residual solution. As the concentration of EDTA increased, the monolith became more compact, and its surface became smoother. Sample f was then chosen for further characterization. The SEM image of sample f (Figure 1g) shows that the monolith possesses a three-dimensional structure consisting of mutual cross-linked corrugated graphene sheets

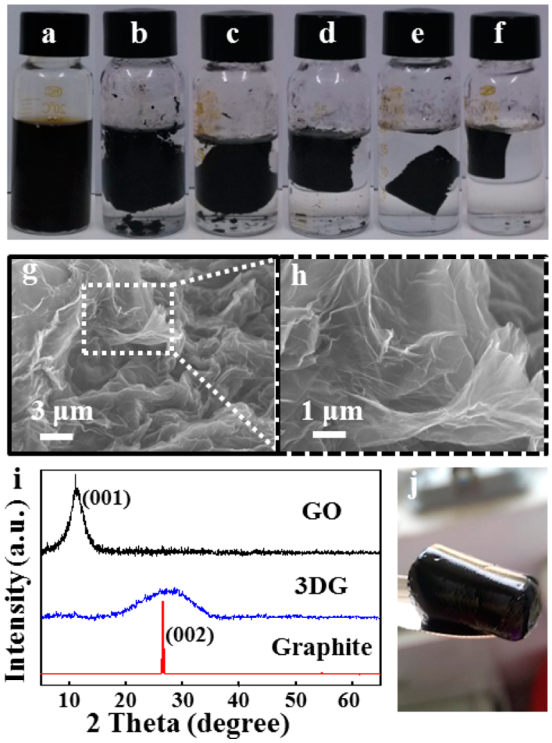


**Figure 1.** (a–f) Photos of 3DG synthesized under 0, 1, 2, 3, 4, and 5 mmol EDTA, respectively, (g and h) SEM images of 3DG; panel h shows the partial enlarged view of panel g. (i) XRD patterns of GO, 3DG, and graphite and (j) a close-up photo of 3DG.

with no obvious orientation, which is in agreement with the existing 3DG reports.[4,11,21,35,36] As can be seen in the magnified image (Figure 1h), the graphene sheets still maintain the layered structure while acting as building blocks, implying possible large specific area of 3DG. Figure 1i compares the XRD patterns of GO, 3DG, and graphite. For GO, a prominent peak of (001) faces exists at 10.99°, corresponding to an interlayer space of 8.05 Å. This peak disappears in the XRD pattern of 3DG, and a broad peak appears instead near the (002) peak of graphite at around 27°, which corresponds to a decreased interlayer space of 3.26 Å. This might be due to the $\pi-\pi$ stacking of graphene sheets during the 3DG assembly.[11,21] Also, the broadness of the peak indicates a disordered orientation of graphene sheets in 3DG, which agrees the SEM results. More structure information is provided in Supporting Information (Figure S1).

Figure 2 shows the $N_2$ adsorption–desorption isotherm results at 77 K. The type IV isotherm curve with a clear type H2 hysteresis loop suggests a complex pore structure in which network effects are important.[37,38] The pore width distribution of 3DG (Figure S2, Supporting Information) showed a wide distribution ranging from 2 to 90 nm which might be due to the randomly self-assembly process. The specific surface area of 3DG, as calculated using a multipoint Brunauer–Emmett–Teller (BET), was 103.5 $m^2\ g^{-1}$, which was a little lower than that of GO (115.0 $m^2\ g^{-1}$ without sonication). All of the results above suggest that the 3DG monolith can preserve the structure advantages of GO, and therefore possibly good adsorption performance.

It can be observed from FTIR spectra (Figure 3a) that three bands of GO, that is, C=O (1725 $cm^{-1}$), C–O–C (1224 $cm^{-1}$), and C–O (1042 $cm^{-1}$), are absent in that of 3DG,

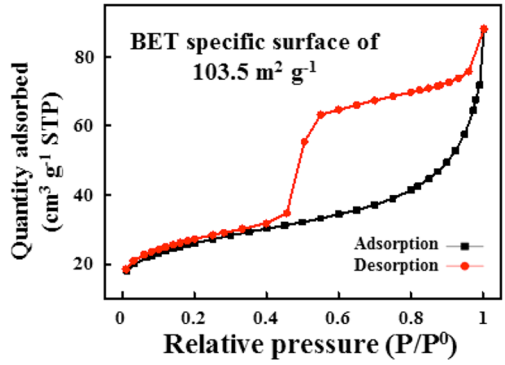


**Figure 2.** $N_2$ adsorption–desorption isotherms at 77 K.

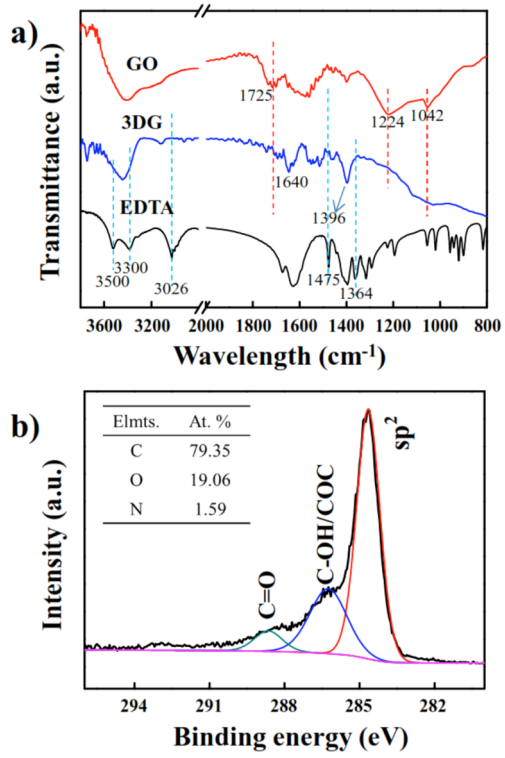


**Figure 3.** (a) FTIR spectra of GO, 3DG, and EDTA and (b) XPS spectra of 3DG.

suggesting the reduction of hydrophilic oxygen-containing groups during synthesis.[35,39] Besides, representative bands of EDTA[40] such as N–H (3500, 3300, and 1364 $cm^{-1}$), O–H (3026 $cm^{-1}$), and C–H (1475 $cm^{-1}$) are also absent in the spectrum of 3DG, indicating little EDTA entered 3DG eventually. It should also be noted that 3DG still maintains some negatively charged oxygen-containing groups such as $COO^-$ (1640 $cm^{-1}$) and $C-O^-$ (1396 $cm^{-1}$). The FTIR results are also confirmed by XPS measurements. The C 1s spectra of 3DG can be deconvoluted into three components: C=C/C–C (284.65 eV), C–O–C/C–OH (286.25 eV), and C=O (288.65 eV).[36,41] The prominent peak representing $sp^2$ C indicates most C atoms are not related to O, which is also proven by the atomic ratio (O/C = 0.24). The extremely low level of N (1.59%) might be due to the trace residue of EDTA.

**3.2. Possible Formation Process and the Reusing of EDTA.** The FTIR and XPS results mentioned above suggest that the process of GO assembly to 3DG is accompanied by the decrease of oxygen-containing groups. Similar to other


dx.doi.org/10.1021/am504922v | ACS Appl. Mater. Interfaces 2014, 6, 19766–19773

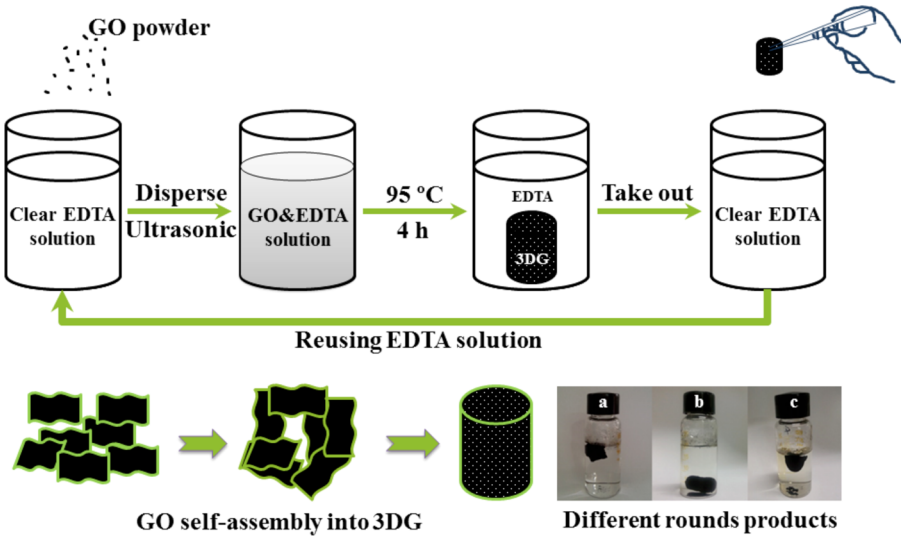


**Figure 4.** Illustration of the EDTA reusing synthetic process, the possible formation process of 3DG, and the photos of 3DG after reusing EDTA solution (a) 1, (b) 5 and (c) 10 times.

assembly methods based on reduction (Figure 4), the decrease of hydrophilic oxygen-containing groups would lower the stability of GO dispersion and cause aggregation. Meanwhile, $\pi-\pi$ interaction and hydrophobic interactions cause the flexible graphene sheets to randomly stack into the 3D monolith structure. In Figure 1a, no aggregation can be observed in the GO solution without EDTA at 95 °C. Therefore, it is proposed that EDTA could cause the reduction of GO and finally the formation of 3DG. The role of EDTA in the 3DG self-assembly was further discussed later in this work.

In addition, it was found that the concentration of EDTA showed no obvious change before and after the synthesis.[42] Thus, EDTA solution was recycled and reused during synthesis. As shown in Figure 4, after one round of synthesis, the 3DG was conveniently removed, and GO powder was added into the EDTA residue solution with sonication before the next round. The picture in Figure 4 shows that complete 3DG can be successively obtained for over 10 times. Reusing EDTA solution can effectively lower the costs, simplify the operation, and improve the applicability.

The above results suggest that 3DG might be a potential adsorbent as a result of its large specific surface area resulting from the mutual cross-linking structure. Paraquat, a highly toxic herbicide, was chosen as a model compound to investigate the adsorption properties of 3DG. Figure 5a shows the molecular structure of paraquat. The two positive charges and delocalized $\pi$ bonds of paraquat may have good interactions with the negatively charged groups of 3DG and its rich delocalized $\pi$ electrons, respectively.

**3.3. Adsorption Isotherm.** The adsorption of paraquat by 0.19 g $L^{-1}$ 3DG at initial concentrations of paraquat from 10 to 400 mg $L^{-1}$ is shown in Figure 5b. To fit the experimental data, two common isotherm models (Langmuir and Freundlich) were adopted here.

Langmuir

$$Q_e = \frac{Q^0 b C_e}{1 + b C_e} \quad (1)$$

Freundlich

$$Q_e = k C_e^{1/n} \quad (2)$$

where $Q_e$ is the amount adsorbed at equilibrium (m $g^{-1}$) and $C_e$ is the equilibrium concentration (mg $L^{-1}$); $Q^0$ is the maximum amount or the saturated adsorption amount (mg $g^{-1}$); $b$ is a constant related to the binding strength (L $mg^{-1}$); and $n$ and $k$ are constants indicative of adsorption intensity and adsorption capacity, respectively. The parameters of adsorption fitting are given in Table S1 (Supporting Information).

As shown in Figure 5b, the Langmuir model is more appropriate and effective than the Freundlich model to depict the adsorption of paraquat by 3DG. This suggests that all the graphene sheets within 3DG possess uniform adsorption activation for paraquat, allowing the formation of a single paraquat molecular layer on graphene sheets without interaction or competition. Also, because of the limited specific surface area and adsorption capacity of 3DG, the Freundlich model is not suitable for its assumed exponential growing capacity. It should be noted that the saturated adsorption capacity of 3DG on paraquat can reach as high as 119 mg $g^{-1}$ (Table S1, Supporting Information) under our experimental conditions. This capacity is much higher than classic paraquat adsorbents, such as clay, earth, and activated carbon (Table 1). Therefore, 3DG is an excellent adsorbent for paraquat with very high capacity.

**3.4. Adsorption Kinetics.** Figure 5c illustrates the kinetic adsorption curve for paraquat with initial concentrations of 50 and 20 mg $L^{-1}$ at 298 K. In the first ~2.5 h, the adsorption at both paraquat concentrations rapidly reaches 90% of their equilibrium adsorption capacities, followed by a slower increase until equilibrium. The high initial adsorption rate indicates that strong interactions exist between 3DG and paraquat. The interactions might result from the electrostatic attraction between the negatively charged oxygen-containing groups of 3DG and the positively charged sites paraquat possesses. $\pi-\pi$ interactions could also contribute since both 3DG and paraquat contain conjugated six-membered rings. A pseudo-second-order model was adopted here to fit the experimental data for the analysis of the rate-limiting step. The equation is expressed as

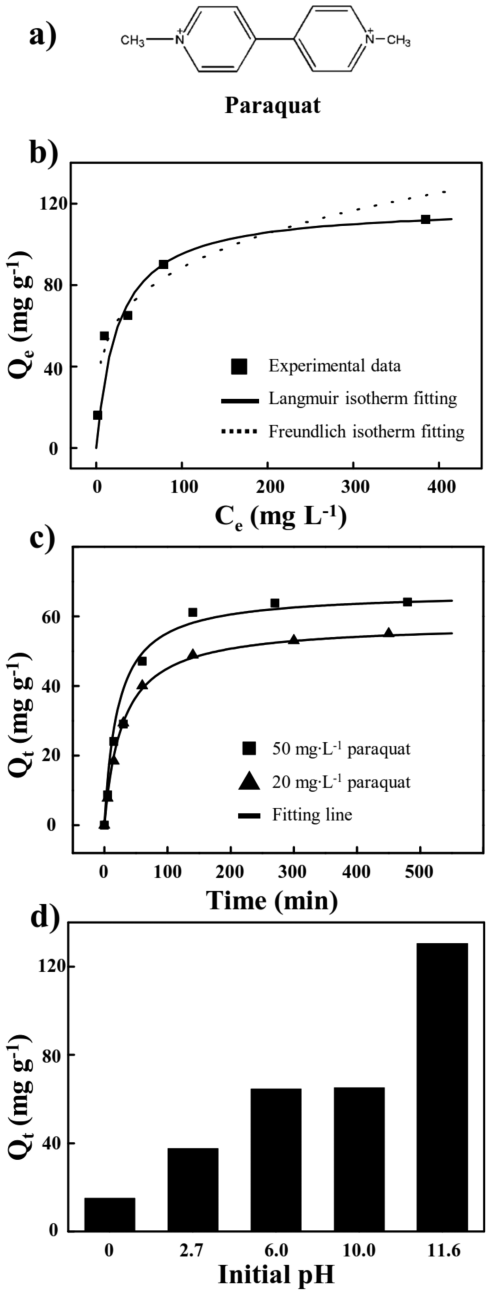


**Figure 5.** (a) Chemical structure of the paraquat molecule; (b) adsorption isotherm experiment and the fitting result by Langmuir and Freundlich isotherm models for 50 mg L$^{-1}$ paraquat adsorbed by 3DG; (c) adsorptions of 20 and 50 mg L$^{-1}$ paraquat on 3DG as a function of contact time and the fitting results by a pseudo second order equation with pH all set to 6; and (d) the adsorption capacities of 3DG for 50 mg L$^{-1}$ paraquat under different pH values. The temperatures were all maintained at 298 K and the dosage of 3DG was 0.19 g L$^{-1}$.

$$\frac{t}{Q_t} = \frac{1}{kQ_e^{\,2}} + \frac{t}{Q_e} \tag{3}$$

where $Q_e$ (mg L$^{-1}$) is the amount of paraquat adsorbed at equilibrium; $Q_t$ is the amount of paraquat adsorbed at contact time $t$ (min); and $k$ (g mg$^{-1}$ min$^{-1}$) is the rate constant of the second-order adsorption. The fitting results and related parameters are shown in Figure 5c and Table 2. It can be observed that for both concentrations, the correlation coefficients ($R^2$) exceed 0.99. The high $R^2$ and the agreement between calculated and experimental $Q_e$ values both suggest that the kinetic adsorption of paraquat on 3DG follows the pseudo-second-order model, implying that the rate-limiting step might be the chemical adsorption step.

**Table 1. Paraquat Adsorption Capacity of Various Inorganic Adsorbents and Clay Minerals**

| adsorbents | $Q^0$ (mg g$^{-1}$) | ref |
|---|---|---|
| activated bleaching earth | 34.965 | 31 |
| activated carbon | 7.51 | 24 |
| clays and organoclays | 51.4 | 29 |
| activated clay | 58.48 | 27 |
| spent and treated diatomaceous earth | 17.06 | 30 |
| modified rice husk | 292.5, 317.7 | 32, 33 |
| zeolite NaY | 185.2 | 26 |
| activated clay | 56.18 | 28 |
| sepiolite | 35.98 | 43 |
| 3DG | 119.0 (pH 6.0), 604.6 (pH 12.0) | this work |

Table 2 shows the initial adsorption rate, $h$ (mg g$^{-1}$ min$^{-1}$), and half-equilibrium time, $t_{1/2}$ (min), with calculation equations shown below:[44,45]

$$h = kQ_e^{\,2} \tag{4}$$

$$t_{1/2} = \frac{1}{kQ_e} \tag{5}$$

where $t_{1/2}$ is the time required for the adsorbent to reach a half-saturation state (when $t = t_{1/2}$, $Q_t = 0.5Q_e$), and is often used as a measure of the adsorption rate. As shown in Table 2, $t_{1/2}$ equals ~24 min under both concentrations, indicating 3DG can quickly remove paraquat from water and reach the half-saturation state within half an hour.

**3.5. Effect of pH.** Figure 5d shows the adsorption results for 50 mg L$^{-1}$ paraquat at 298 K at various initial pH values (0, 2.7, 6.0, 10.0 and 11.6). At pH 0, the adsorption capacity is rather low (~15 mg L$^{-1}$). As the solution rises to neutral or weak alkaline pH, the adsorption capacity also gradually increases (~68 mg L$^{-1}$). Adsorption abruptly rises when the pH reaches the strong alkalinity region (~130 mg L$^{-1}$). It is proposed that at lower pH, the abundant $H^+$ existing in solution would tend to protonate the active adsorption sites ($-COO^-$, $-O^-$) and compete with paraquat, causing a lower adsorption capacity. When the pH starts to rise, the competition from $H^+$ decreases, in favor of a higher adsorption capacity. When the solution is strongly basic, most of the active sites in graphene sheets are deprotonated, in favor of paraquat binding at its positively charged sites resulting in extra large adsorption capacity.

**3.6. Recycling of Paraquat Using a 3DG Teabag.** Based on the above findings that little paraquat can be adsorbed on 3DG in a very acidic solution, a solution of pH = 0 was adopted here for the desorption experiment. To simplify the recycling process and take advantage of the monolith 3DG in easy separation, a 3DG teabag method is shown in Figure 6.

Unlike other powdered adsorbents, 3DG can keep its monolith structure during adsorption. Therefore, a pyramid-shaped teabag was chosen to make the 3DG teabag (Figure 6). The teabag has a regular tetrahedron structure and is made of food-level nylon. Because the teabag has sufficient space and

Table 2. Kinetic Parameters for the Adsorption of 20 and 50 mg $L^{-1}$ Paraquat Fitting by Pseudo Second Order Equation

| initial $C_0$ (mg $L^{-1}$) | $Q_e$ (mg $g^{-1}$) | k (g $mg^{-1}$ $min^{-1}$) | $R^2$ | $h$ (mg $g^{-1}$ $min^{-1}$) | $t_{1/2}$ (min) |
|---|---|---|---|---|---|
| 20 | 57.47 | 0.00073 | 0.9961 | 2.41 | 23.86 |
| 50 | 68.03 | 0.00062 | 0.9947 | 2.88 | 23.61 |

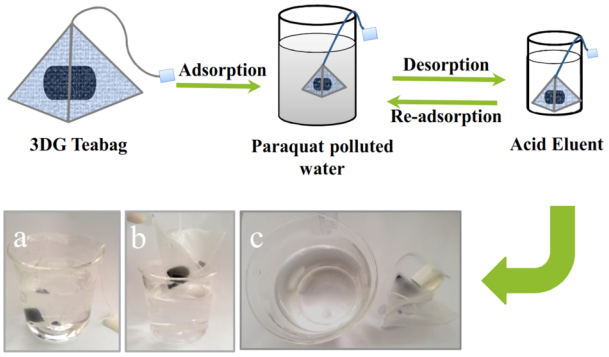


Figure 6. Illustration of the recycling process using a 3DG teabag and the photo of actual (a) adsorption, (b) direct separation, and (c) the clear adsorbed solution.

the teabag wall is webbed, the enclosed 3DG has enough active space without being compressed and the solution has free access to the 3DG through the webbed wall. As shown in Figure 6a, since the teabag protects the 3DG from direct contact with the magnetic stirrer, stirring causes minimal damage. After reaching equilibrium, the adsorbent can be separated from the solution simply by lifting out the 3DG teabag (Figure 6b). After separation, the solution is clear without any graphene sheets left (Figure 6c) and the teabag can be directly used into the next desorption and recycling cycle. No traditional separation methods such as precipitation, filtration, and centrifugation are needed, which is certainly more convenient and energy-efficient. Unlike the method of using magnetic iron cores, this teabag system is well suited for treating acidic samples or recycling systems involving acidic eluent due to the acid-tolerance of the nylon material. Control experiment was performed to exclude the effect of nylon teabag, and the teabag showed no adsorption effect to paraquat.

As shown in Figure 7, the adsorption capacity of 3DG teabag only decreased from 155 mg $g^{-1}$ to 136 mg $g^{-1}$ after five cycles. Also, Figure 6b shows that after the recycling, the teabag can still protect the monolith structure of 3DG. Detailed structure information is provided in Figure S3 (Supporting Information).

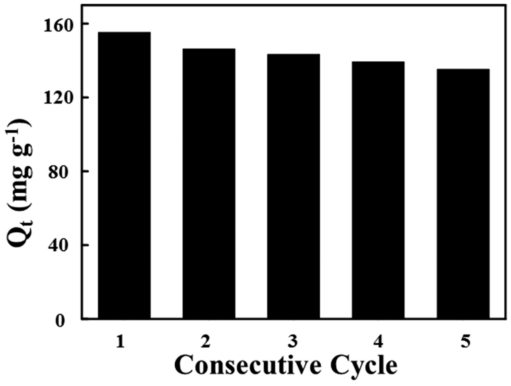


Figure 7. Recycling of 3DG in the removal of paraquat. Conditions: the pH values of the paraquat solution and the acid eluent are 12.0 and 0, respectively; $T$ = 298 K; 0.19 g $L^{-1}$ 3DG.

### 3.7. The Role of EDTA in the Self-Assembly Process.

The results in Figure 3 reveal that very little EDTA or its derivant were in the final product, which means EDTA may not act as a linking agent here. Also, the similar shapes of three samples in Figure S4 (Supporting Information) indicate that EDTA did not decompose during the self-assembly process, meaning it might not play as a regular reduction agent either. Actually, the linking agent or classic reduction agent is not always necessary in 3DG synthesis. Shi et al.[18] developed a well-known hydrothermal method of using only pure water and GO to obtain 3DG structure at 180 °C. They found the oxygen-obtained groups on GO were reduced during synthesis and suggested this is the key of the 3DG assembly. Zhou et al.[46] also proposed a "water-only" route by hydrothermal treatment of GO solutions even earlier. They believed that the reduction process is analogous to the $H^+$-catalyzed dehydration of alcohol, where water acts as a source of $H^+$ for the protonation of hydroxyl groups. Their results also suggest that a basic solution yields a stable rGO solution while an acidic solution results in aggregation of rGO sheets.

EDTA owns abundant −COOH, which could be the source of $H^+$ for the protonation of hydroxyl groups together with water. The presence of EDTA helps ease the original harsh experiment condition (high pressure, high temperature) by making $H^+$ easier to be "activated". Because EDTA only provides $H^+$ during synthesis, it would not form any conjugated bonds with graphene or enter the 3DG structure eventually. This might also explain why EDTA consumes so little and can be recycled during synthesis. Moreover, EDTA also ensures an acidic synthesis environment, leading reduced graphene sheets assembled into a stable 3D structure. Therefore, we suggest that EDTA acts as a "catalyst" of the 3DG formation process. A scheme of the possible mechanisms was proposed in Scheme S1 (Supporting Information).

## 4. CONCLUSION

A mild synthetic method for 3DG monolith was developed in this work through an EDTA-induced GO self-assembly process at 95 °C. Because little EDTA was consumed in this process, EDTA solution was reused more than 10 times, which effectively could lower the costs. In the removal of paraquat, 3DG was found to be an excellent adsorbent with superior adsorption capacity of 119 mg $g^{-1}$ (pH 6.0), much higher than those in existing reports. Finally, a 3DG teabag adsorbent was made and applied in the adsorption−desorption process. After five cycles, 88% adsorption capacity still remained. The 3DG teabag method is a facile method with potential applications in many other systems.

## ■ ASSOCIATED CONTENT

### Ⓢ Supporting Information

Photographs and SEM and TEM images of 3DG before and after adsorption, Langmuir and Freundlich constants associated with adsorption isotherms of 3DG on paraquat, the pore size distribution of 3DG, the FTIR results of pure EDTA solution

and reaction solution before and after 3DG synthesis, and the possible formation process of 3DG catalyzed by EDTA. This material is available free of charge via the Internet at http://pubs.acs.org.

## AUTHOR INFORMATION


### Corresponding Author

*E-mail: zlin@fjirsm.ac.cn. Tel./Fax: (+086)591-83705474.


### Notes

The authors declare no competing financial interest.

## ACKNOWLEDGMENTS

Financial support was provided by the National Basic Research Program of China (2010CB933501, 2013CB934302, 2014CB932101), the Outstanding Youth Fund (21125730), the National Science Foundation Grant (21273237, 21307130, 21477129), the "Strategic Priority Research Program" of the Chinese Academy of Sciences (XDA09030203), the Knowledge Innovation Program of the Chinese Academy of Sciences (KJCX2-YW-N50, KJCX2EW-J02), and the Fund of Fujian Key Laboratory of Nanomaterials (2006L2005).

## REFERENCES


(1) Cao, X.; Yin, Z.; Zhang, H. Three-Dimensional Graphene Materials: Preparation, Structures and Application in Supercapacitors. *Energy Environ. Sci.* **2014**, *7*, 1850−1865.

(2) Chabot, V.; Higgins, D.; Yu, A.; Xiao, X.; Chen, Z.; Zhang, J. A Review of Graphene and Graphene Oxide Sponge: Material Synthesis and Applications to Energy and the Environment. *Energy Environ. Sci.* **2014**, *7*, 1564−1596.

(3) Niu, Z.; Liu, L.; Zhang, L.; Shao, Q.; Zhou, W.; Chen, X.; Xie, S. A Universal Strategy to Prepare Functional Porous Graphene Hybrid Architectures. *Adv. Mater.* **2014**, *26*, 3681−3687.

(4) Zhao, Y.; Hu, C.; Song, L.; Wang, L.; Shi, G.; Dai, L.; Qu, L. Functional Graphene Nanomesh Foam. *Energy Environ. Sci.* **2014**, *7*, 1913−1918.

(5) Mi, X.; Huang, G.; Xie, W.; Wang, W.; Liu, Y.; Gao, J. Preparation of Graphene Oxide Aerogel and Its Adsorption for $Cu^{2+}$ Ions. *Carbon* **2012**, *50*, 4856−4864.

(6) Chen, Y.; Chen, L.; Bai, H.; Li, L. Graphene Oxide−Chitosan Composite Hydrogels as Broad-Spectrum Adsorbents for Water Purification. *J. Mater. Chem. A* **2013**, *1*, 1992−2001.

(7) Chen, S.; He, G.; Hu, H.; Jin, S.; Zhou, Y.; He, Y.; He, S.; Zhao, F.; Hou, H. Elastic Carbon Foam Via Direct Carbonization of Polymer Foam for Flexible Electrodes and Organic Chemical Absorption. *Energy Environ. Sci.* **2013**, *6*, 2435−2439.

(8) Jiang, L.; Fan, Z. Design of Advanced Porous Graphene Materials: From Graphene Nanomesh to 3D Architectures. *Nanoscale* **2014**, *6*, 1922−1945.

(9) Bi, H.; Xie, X.; Yin, K.; Zhou, Y.; Wan, S.; He, L.; Xu, F.; Banhart, F.; Sun, L.; Ruoff, R. S. Spongy Graphene as a Highly Efficient and Recyclable Sorbent for Oils and Organic Solvents. *Adv. Funct. Mater.* **2012**, *22*, 4421−4425.

(10) Xue, Z.; Cao, Y.; Liu, N.; Feng, L.; Jiang, L. Special Wettable Materials for Oil/Water Separation. *J. Mater. Chem. A* **2014**, *2*, 2445−2460.

(11) Wang, J.; Shi, Z.; Fan, J.; Ge, Y.; Yin, J.; Hu, G. Self-Assembly of Graphene into Three-Dimensional Structures Promoted by Natural Phenolic Acids. *J. Mater. Chem.* **2012**, *22*, 22459−22466.

(12) Wei, G.; Miao, Y. E.; Zhang, C.; Yang, Z.; Liu, Z.; Tjiu, W. W.; Liu, T. Ni-Doped Graphene/Carbon Cryogels and Their Applications as Versatile Sorbents for Water Purification. *ACS Appl. Mater. Interfaces* **2013**, *5*, 7584−7591.

(13) Xu, L.; Liu, N.; Cao, Y.; Lu, F.; Chen, Y.; Zhang, X.; Feng, L.; Wei, Y. Mercury Ion Responsive Wettability and Oil/Water Separation. *ACS Appl. Mater. Interfaces* **2014**, *6*, 13324−13329.

(14) Xu, L.; Zhang, X.; Zhu, C.; Zhang, Y.; Fu, C.; Yang, B.; Tao, L.; Wei, Y. Nonionic Polymer Cross-Linked Chitosan Hydrogel: Preparation and Bioevaluation. *J. Biomater. Sci. Polym. Ed.* **2013**, *24*, 1564−1574.

(15) Zhang, H. B.; Wang, J. W.; Yan, Q.; Zheng, W. G.; Chen, C.; Yu, Z. Z. Vacuum-Assisted Synthesis of Graphene from Thermal Exfoliation and Reduction of Graphite Oxide. *J. Mater. Chem.* **2011**, *21*, 5392−5397.

(16) Peng, Z.; Yan, Z.; Sun, Z.; Tour, J. M. Direct Growth of Bilayer Graphene on $SiO_2$ Substrates by Carbon Diffusion through Nickel. *ACS Nano* **2011**, *5*, 8241−8247.

(17) Chen, Z.; Ren, W.; Gao, L.; Liu, B.; Pei, S.; Cheng, H. M. Three-Dimensional Flexible and Conductive Interconnected Graphene Networks Grown by Chemical Vapour Deposition. *Nat. Mater.* **2011**, *10*, 424−428.

(18) Xu, Y.; Sheng, K.; Li, C.; Shi, G. Self-Assembled Graphene Hydrogel Via a One-Step Hydrothermal Process. *ACS Nano* **2010**, *4*, 4324−4330.

(19) Zhao, J.; Ren, W.; Cheng, H. M. Graphene Sponge for Efficient and Repeatable Adsorption and Desorption of Water Contaminations. *J. Mater. Chem.* **2012**, *22*, 20197−20202.

(20) Zhao, Y.; Liu, J.; Hu, Y.; Cheng, H.; Hu, C.; Jiang, C.; Jiang, L.; Cao, A.; Qu, L. Highly Compression-Tolerant Supercapacitor Based on Polypyrrole-Mediated Graphene Foam Electrodes. *Adv. Mater.* **2013**, *25*, 591−595.

(21) Chen, W.; Yan, L. In Situ Self-Assembly of Mild Chemical Reduction Graphene for Three-Dimensional Architectures. *Nanoscale* **2011**, *3*, 3132−3137.

(22) Fernández-Merino, M. J.; Guardia, L.; Paredes, J. I.; Villar-Rodil, S.; Solís-Fernández, P.; Martínez-Alonso, A.; Tascón, J. M. D. Vitamin C Is an Ideal Substitute for Hydrazine in the Reduction of Graphene Oxide Suspensions. *J. Phy. Chem. C* **2010**, *114*, 6426−6432.

(23) Gui, X.; Zeng, Z.; Lin, Z.; Gan, Q.; Xiang, R.; Zhu, Y.; Cao, A.; Tang, Z. Magnetic and Highly Recyclable Macroporous Carbon Nanotubes for Spilled Oil Sorption and Separation. *ACS Appl. Mater. Interfaces* **2013**, *5*, 5845−5850.

(24) Hamadi, N. K.; Sri, S.; Chen, X. D. Adsorption of Paraquat Dichloride from Aqueous Solution by Activated Carbon Derived from Used Tires. *J. Hazard. Mater.* **2004**, *112*, 133−141.

(25) Ritter, L.; Solomon, K.; Sibley, P.; Hall, K.; Keen, P.; Mattu, G.; Linton, B. Sources, Pathways, and Relative Risks of Contaminants in Surface Water and Ground Water: A Perspective Prepared for the Walkerton Inquiry. *J. Toxicol. Environ. Health, Part A* **2002**, *65*, 1−142.

(26) Rongchapo, W.; Sophiphun, O.; Rintramee, K.; Prayoonpokarach, S.; Wittayakun, J. Paraquat Adsorption on Porous Materials Synthesized from Rice Husk Silica. *Water Sci. Technol.* **2013**, *68*, 863−869.

(27) Tsai, W. T.; Lai, C. W.; Hsien, K. J. Effect of Particle Size of Activated Clay on the Adsorption of Paraquat from Aqueous Solution. *J. Colloid Interface Sci.* **2003**, *263*, 29−34.

(28) Tsai, W. T.; Lai, C. W.; Hsien, K. J. The Effects of pH and Salinity on Kinetics of Paraquat Sorption onto Activated Clay. *Colloids Surf., A* **2003**, *224*, 99−105.

(29) Seki, Y.; Yurdakoc, K. Paraquat Adsorption onto Clays and Organoclays from Aqueous Solution. *J. Colloid Interface Sci.* **2005**, *287*, 1−5.

(30) Tsai, W. T.; Hsien, K. J.; Chang, Y. M.; Lo, C. C. Removal of Herbicide Paraquat from an Aqueous Solution by Adsorption onto Spent and Treated Diatomaceous Earth. *Bioresour. Technol.* **2005**, *96*, 657−663.

(31) Tsai, W. T.; Lai, C. W.; Hsien, K. J. Adsorption Kinetics of Herbicide Paraquat from Aqueous Solution onto Activated Bleaching Earth. *Chemosphere* **2004**, *55*, 829−837.

(32) Hsu, S. T.; Pan, T. C. Adsorption of Paraquat Using Methacrylic Acid-Modified Rice Husk. *Bioresour. Technol.* **2007**, *98*, 3617−3621.

(33) Hsu, S. T.; Chen, L. C.; Lee, C. C.; Pan, T. C.; You, B. X.; Yan, Q. F. Preparation of Methacrylic Acid-Modified Rice Husk Improved by an Experimental Design and Application for Paraquat Adsorption. *J. Hazard. Mater.* **2009**, *171*, 465−470.

(34) Hummers, W. S.; Offeman, R. E. Preparation of Graphitic Oxide. *J. Am. Chem. Soc.* **1958**, *80*, 1339−1339.
(35) Zhang, L.; Wang, T.; Wang, H.; Meng, Y.; Yu, W.; Chai, L. Graphene@Poly(*m*-phenylenediamine) Hydrogel Fabricated by a Facile Post-Synthesis Assembly Strategy. *Chem. Commun.* **2013**, *49*, 9974−9976.
(36) Zhang, L.; Chen, G.; Hedhili, M. N.; Zhang, H.; Wang, P. Three-Dimensional Assemblies of Graphene Prepared by a Novel Chemical Reduction-Induced Self-Assembly Method. *Nanoscale* **2012**, *4*, 7038−7045.
(37) Li, B. J.; Cao, H. Q.; Yin, G. Mg(OH)(2)@Reduced Graphene Oxide Composite for Removal of Dyes from Water. *J. Mater. Chem.* **2011**, *21*, 13765−13768.
(38) Thommes, M. Physical Adsorption Characterization of Nanoporous Materials. *Chem. Ing. Technol.* **2010**, *82*, 1059−1073.
(39) Pei, S.; Cheng, H.-M. The Reduction of Graphene Oxide. *Carbon* **2012**, *50*, 3210−3228.
(40) Lanigan, K. C.; Pidsosny, K. Reflectance FTIR Spectroscopic Analysis of Metal Complexation to EDTA and EDDS. *Vib. Spectrosc.* **2007**, *45*, 2−9.
(41) Zhang, J.; Yang, H.; Shen, G.; Cheng, P.; Zhang, J.; Guo, S. Reduction of Graphene Oxide Vial-Ascorbic Acid. *Chem. Commun.* **2010**, *46*, 1112−1114.
(42) Cagnasso, C. E.; Lopez, L. B.; Rodriguez, V. G.; Valencia, M. E. Development and Validation of a Method for the Determination of EDTA in Non-Alcoholic Drinks by HPLC. *J. Food Compos. Anal.* **2007**, *20*, 248−251.
(43) Rytwo, G.; Tropp, D.; Serban, C. Adsorption of Diquat, Paraquat and Methyl Green on Sepiolite: Experimental Results and Model Calculations. *Appl. Clay Sci.* **2002**, *20*, 273−282.
(44) Demirbaş, Ö.; Turhan, Y.; Alkan, M. Thermodynamics and Kinetics of Adsorption of a Cationic Dye onto Sepiolite. *Desalin. Water Treat.* **2014**, 1−8.
(45) Cao, Q.; Huang, F.; Zhuang, Z.; Lin, Z. A Study of the Potential Application of Nano-$Mg(OH)_2$ in Adsorbing Low Concentrations of Uranyl Tricarbonate from Water. *Nanoscale* **2012**, *4*, 2423−2430.
(46) Zhou, Y.; Bao, Q.; Tang, L. A. L.; Zhong, Y.; Loh, K. P. Hydrothermal Dehydration for the "Green" Reduction of Exfoliated Graphene Oxide to Graphene and Demonstration of Tunable Optical Limiting Properties. *Chem. Mater.* **2009**, *21*, 2950−2956.